Available online at www.sciencedirect.com
SCIENCE DIRECT®
Journal of Solid State Chemistry 173 (2003) 130–136
JOURNAL OF SOLID STATE CHEMISTRY
http://elsevier.com/locate/jssc

Structural characterization and physical properties of the system $La_{1.33}Li_xCr_xTi_{2-x}O_6$

A.I. Ruiz,[a,*] M.L. López,[a] C. Pico,[a] A. Santrich-Badal,[b] and M.L. Veiga[a]

[a] *Departamento Química Inorgánica I, Facultad de Ciencias Químicas, Universidad Complutense, 28040 Madrid, Spain*
[b] *Departamento de Propiedades Ópticas, Magnéticas y de Transporte, Instituto Ciencia de Materiales, Consejo Superior de Investigaciones Científicas, Cantoblanco, 28049 Madrid, Spain*

Received 19 November 2002; received in revised form 14 January 2003; accepted 18 January 2003

Abstract

New phases which arise from partial substitution of Ti^{4+} by Cr^{3+} and Li^+ of the compound $La_{2/3}TiO_3$ have been obtained, giving rise to the series $La_{1.33}Li_xCr_xTi_{2-x}O_6$ ($x = 0.66$, 0.55 and 0.44). These phases adopt a perovskite-type structure as deduced from their structural characterization. Rietveld's analyses of neutron diffraction data show that it is orthorhombic (*S.G. Pbnm*) with ordered domains. Conductivity has been examined by complex impedance spectroscopy and it increases with increasing lithium and chromium content. These materials behave as mixed conductors with low activation energies. Magnetic susceptibility variation with temperature shows antiferromagnetic interactions at the lowest temperatures.

Keywords: Perovskite phases; Neutron diffraction; Semiconductors; Magnetic properties

1. Introduction

Materials with perovskite-type structure and related oxides of the first transition metals are attractive candidates for a great variety of applications (semiconductors, sensors, cathode materials, etc.).

As follows from literature data that the compound $La_{4/3}Ti_2O_6$ [2,3] shows a defect perovskite structure, where only 2/3 of *A*-sites are occupied and 1/3 of them are vacant. These vacancies can be occupied by Li or Na obtaining compounds of general formula $La_{1.33-x}A_{3x}Ti_2O_6$ [4–13], but another possibility is the partial substitution of titanium by a trivalent cation (Cr, Mn or Fe) and a monovalent cation (Li and Na).

In this way, $La_{4/3}Li_{2x}Fe_{2x}Ti_{2-2x}O_6$ [14] has been prepared, and it is observed that the structure stands in a symmetry evolution (orthorhombic–tetragonal) with the composition, leading to the existence of one phase which shows a mixture of both symmetries, but in this series the electrical and magnetic experiments were not performed.

Recently, the study of titanium substitution by Mn or Cr systems have led to compounds of the series $La_{1+2x+2y}Li_{1-6x}Ti_{2-6y}M_{6y}O_6$ [15–18] which show three polymorphs: A, β and C, with different symmetries (cubic, tetragonal and orthorhombic, respectively). These kind of compounds showed both electronic and Li-ion conductivity, and the ionic conductivity was similar in manganese and chromium systems but the electronic conductivity was much higher in the manganese system. Besides, electrochemical insertion and deinsertion have been carried out for samples of chromium leading to the reduction of Cr^{6+} to Cr^{3+} (by means of the interpretation of the authors [18]). The presence of chromium in two different states is the origin of the electronic conductivity in this series.

Finally, we have recently reported some results on the structure, electrical and magnetic behavior of the series $La_{1.33}Na_xMn_xTi_{2-x}O_6$ [19–21]. Samples belonging to this system present orthorhombic ($x = 0.66$) or rhombohedral ($x = 0.55$ and 0.44) symmetry, are electronic ($x = 0.66$) and mixed conductors ($x = 0.55$ and 0.44), and all the samples behave as spin glass due to the magnetic dilution.

The present paper deals with the structural characterization by X-ray and neutron diffraction as well as the

*Corresponding author.
E-mail address: anairuiz@quim.ucm.es (A.I. Ruiz).

0022-4596/03/$ - see front matter © 2003 Elsevier Science (USA). All rights reserved.
doi:10.1016/S0022-4596(03)00104-X

conductivity and magnetic properties of the new phases $La_{1.33}Li_xCr_xTi_{2-x}O_6$ ($x = 0.66$, 0.55 and 0.44).

2. Experimental section

Polycrystalline samples of general composition $La_{1.33}Li_xCr_xTi_{2-x}O_6$ ($x = 0.66$, 0.55 and 0.44) were prepared by a solid-state reaction, from powdered mixtures of $La(NO_3)_3 \cdot 6H_2O$, $LiNO_3$, $C_{15}H_{21}CrO_6$ (chromium (III) acetylacetonate) and $C_{10}H_{14}O_5Ti$ (titanyl acetylacetonate), in stoichiometric ratio. Each mixture was first heated in air at 723 K and followed by a further thermal treatment at 1173 K for 24 h.

X-ray powder diffraction patterns were registered by means of a Siemens Kristallofex diffractometer powered with a D-500 generator using Ni-filtered Cu$K\alpha$ radiation and 2θ step size of 0.05°, with a counting time of 12.5 s for each step. The goniometer was connected to a PC controlled by the commercial program PC-APD (Analytical Powder Diffraction Software, 4.0). The neutron powder diffraction data were recorded on the D1A high-resolution powder diffractometer ($\lambda = 1.9110$ Å) at the Institut Laue-Langevin (Grenoble, France). The neutron and X-ray diffraction patterns were analyzed by the Rietveld method and the Fullprof program [1]. The multidetector D1B powder diffractometer with a wavelength of 2.52 Å was used for the thermal dependence of the diffraction patterns in the 1.6–300 K temperature range.

Electrical measurements were carried out using a Solartron 1260 Impedance/Gain Phase Analyzer in the 0.1 Hz–10 MHz frequency range with 0.05 V. Samples were pressed into pellets, with a geometrical factor l/A close to 3 cm^{-1}, and then sintered in air at 1173 K for 48 h. Blocking electrodes were deposited on both sides of the pellets by platinum paint. Resistance values were derived from an interpretation of the complex impedance plane diagram of the data.

Charge/discharge experiments on cells consisting of pellets sandwiched between blocking platinum electrodes, showed that significant amounts of current could be passed on the charging cycle but another considerable amount is also detected, on subsequently placing the cell in the discharge mode. Polarization experiments in d.c. were carried out at 673 K with a charging voltage of 1 V for the compositions $x = 0.66$, 0.55 and 0.44. These samples and electrodes were the same as those used for conductivity measurements. The equipment includes a standard resistor that was in series with the sample during charging and discharging cycles.

Magnetic measurements were obtained in a SQUID (Quantum Design, MPMS-XL model) with a sensitivity of 10^{-10} emu in the temperature range 2–600 K, applying a field of 5000 and 50 Oe.

3. Results and discussion

3.1. Structural analysis

In the $La_{1.33}Li_xCr_xTi_{2-x}O_6$ ($x = 0.66$, 0.55 and 0.44) series there is no change in the La content. The charge balance modification induced by the partial substitution for Ti^{4+} with Cr^{3+} being corrected by Li^+ ions addition.

X-ray and neutron diffraction patterns showed that in this series a perovskite-type structure is stabilized, and the Bragg peaks are indexed in an orthorhombic with space group *Pbnm* cells which show dimensions $a \approx b \approx \sqrt{2}a_p$ and $c \approx 2a_p$, where a_p is an idealized cubic perovskite cell of about 3.9 Å. The results are presented in Fig. 1 for $x = 0.66$ and 0.44, and it can be observed that the *R*-factors are high although they are inside allowed limits to consider the structural model as valid. The observed profiles, calculated profiles and difference neutron diffraction profiles are shown in Fig. 1a and b and a close examination of the profiles revealed that around $2\theta \approx 32°$, the reflection (111) is deviated from the difference line can be observed. In general, the intensity of this reflection is higher when the structure presents order by the planes around *c*-axis, and this peak is

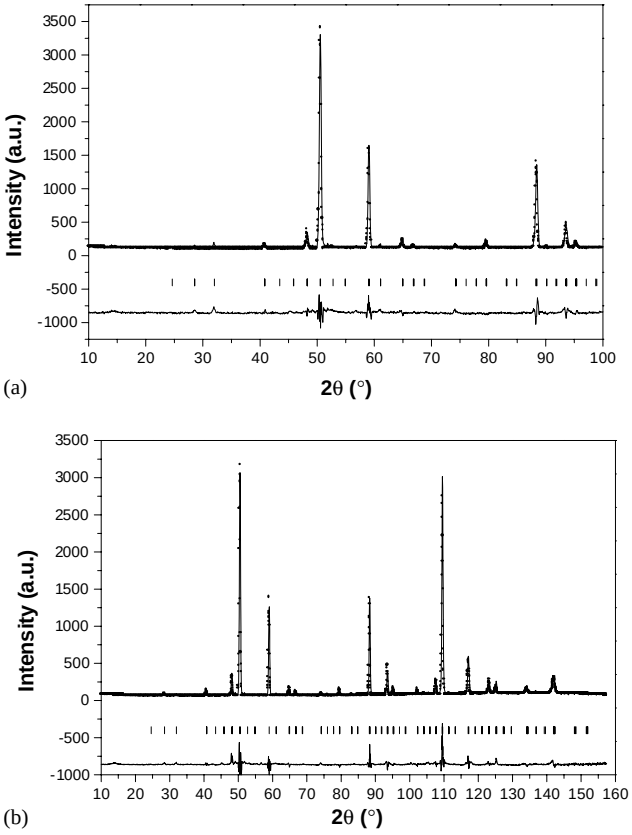

Fig. 1. Calculated and observed neutron diffraction patterns and difference spectrum with space group *Pbnm* for: (a) $La_{1.33}Li_{0.66}Cr_{0.66}Ti_{1.34}O_6$ ($R_p = 9.43$; $R_{wp} = 12.4$; $R_B = 8.85$); and (b) $La_{1.33}Li_{0.44}Cr_{0.44}Ti_{1.56}O_6$ ($R_p = 8.98$; $R_{wp} = 12.7$; $R_B = 8.42$).

usually linked to the reflection (001) that appears around $2\theta \approx 14^\circ$ [8,10,12], which appears in our samples with low intensity. These superstructure lines are the same those observed for the series $La_{1.33-x}Li_{3x}Ti_2O_6$. For these reasons, it is reasonable to think granting the possibility of the existence of order into the structure, but due to the low intensity of the maximum that present the samples of Cr, the order is due to the presence of small domains with a local-order structure. For this reason, the structural refinement must be realized with two "phases", *Pbnm* and *P*4/*mmm* (Fig. 2a and b). For $x = 0.44$ sample, an experimental intensity can be observed and that corresponds to $2\theta \approx 47.5^\circ$, which is higher than the calculated one. However, this fact is justified by the furnace profile (inset Fig. 2b).

Table 1 presents crystallographic data and *R*-factors obtained in the refinements of neutron diffraction for $x = 0.66$ and 0.44. The variation of the cell parameters with the composition is practically useless, and this fact can be mainly attributed to the similar ionic radii between the two cations Ti^{4+} (0.605 Å) and Cr^{3+} (0.60 Å). Also, the refinement of X-ray diffraction data of $x = 0.55$ sample have been carried out, obtaining similar results.

Selected interatomic distances and angles from the refined atomic positions are listed in Table 2, and they show that the samples of this system present a perovskite-type structure (Fig. 3) with a distance mean of similar values for the different compositions and close to the sum of the ionic radii [22]. The tilting of $(Ti/Cr)O_6$ octahedra is small about the directions [001] and [110] (between 8.5° and 6.5°, and 5.5° and 4.5°, respectively). A regular six-coordination for Cr/Ti and a quite distorted 12-coordinated polyhedron for La and Li is found, in spite of the fact that generally the space group *Pbnm* presents an *A* coordination number of 8 due to the tilting octahedra but in this case, the distortion is small because the parameters *a* and *b* are very similar. This behavior can be attributed to the existence of small domains with a local-order structure.

3.2. Electrical properties

Measurements of a.c. impedance spectra have been carried out by alternating current techniques from the complex impedance plots. The main reason for using this method is that the contact and interfacial effects make it difficult to determine the d.c. conductivity directly.

The Z'' (imaginary) against Z' (real) plots at three different temperatures are shown for $x = 0.66$ (Fig. 4). The impedance graphs obtained are very similar for all the samples and they are clearly depressed below the baseline, which is the a consequence of universal response of these materials [23]. In Fig. 4, two semi-circles, with capacitance values of $\approx 1.0 \times 10^{-11}$ and

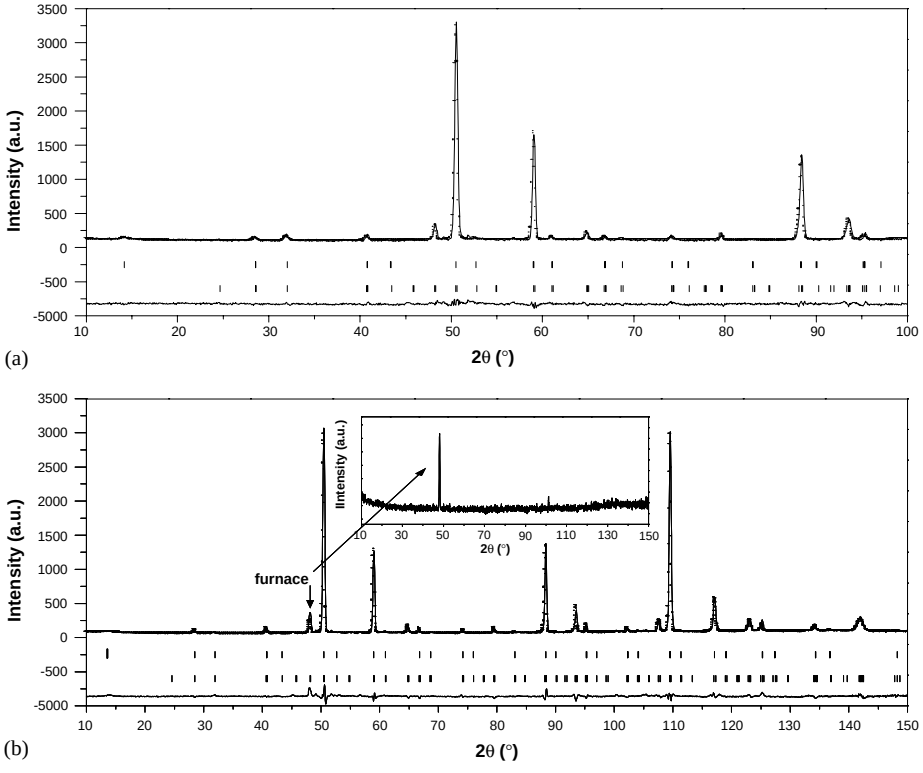

Fig. 2. Calculated and observed neutron diffraction patterns and difference spectrum for: (a) $La_{1.33}Li_{0.66}Cr_{0.66}Ti_{1.34}O_6$ and (b) $La_{1.33}Li_{0.44}Cr_{0.44}Ti_{1.56}O_6$ supposing two phases (*P*4/*mmm* and *Pbnm*). The inset shows the ND patterns of the furnace where it is made collecting data.

Table 1
Refined lattice parameters, atomic positions and *R*-factors for the system $La_{1.33}Li_xCr_xTi_{2-x}O_6$ (*Pbnm* and *P*4/*mmm*) by neutron diffraction

		$x = 0.66$		$x = 0.44$	
	S.G.	*Pbnm*	*P*4/*mmm*	*Pbnm*	*P*4/*mmm*
	a (Å)	5.5045(6)	3.8766(7)	5.4937(1)	3.8787(6)
	b (Å)	5.4739(9)		5.4781(3)	
	c (Å)	7.7477(2)	7.7541(2)	7.7562(5)	7.7560(2)
	V (Å^3)	233.44(3)	116.53(1)	233.48(4)	116.74(6)
(La/)Li)1	*x*	0.0018(4)	0.0000	0.0001(5)	0.0000
	y	0.0014(4)	0.0000	−0.0009(4)	0.0000
	z	0.2500	0.0000	0.2500	0.0000
	Occup.	2.66/1.32	0.48/0.19	2.66/0.88	0.50/0.17
(La/Li)2	*x*	0.0000	0.0000	0.0000	0.0000
	y	0.5000	0.0000	0.5000	0.0000
	z	0.0000	0.5000	0.0000	0.5000
	Occup.	1.32/2.68	0.85/0.47	0.88/3.12	0.83/0.27
Cr/Ti	*x*	0.0000	0.5000	0.0000	0.5000
	y	0.5000	0.5000	0.5000	0.5000
	z	0.0000	0.2794(6)	0.0000	0.2484(6)
	Occup.	1.32/2.68	1.56/0.44	0.88/3.12	1.56/0.44
O1	*x*	0.0536(4)	0.0000	−0.0449(7)	0.0000
	y	0.4998(9)	0.5000	0.4889(2)	0.5000
	z	0.2500	0.2552(2)	0.2500	0.2569(1)
	occup.	4.00	4.00	4.00	4.00
O2	*x*	0.7605(1)	0.5000	0.7474(1)	0.5000
	y	0.2411(1)	0.5000	0.2523(7)	0.5000
	z	−0.0509(7)	0.0000	−0.0233(3)	0.0000
	Occup.	8.00	1.00	8.00	1.00
O3	*x*		0.5000		0.5000
	y		0.5000		0.5000
	z		0.5000		0.5000
	Occup.		1.00		1.00
	R_p (%)		6.58		7.20
	R_{wp} (%)		8.91		10.2
	R_{exp} (%)		5.62		3.90
	R_B (%)	10.6	5.74	6.87	8.66

Table 2
Main interatomic distances (Å) and angles (deg.) for $La_{1.33}Li_xCr_xTi_{2-x}O_6$

Bond atoms	$x = 0.66$	$x = 0.44$
d (La/Li–O1)	2.870(6) × 2	2.885(6) × 2
	2.848(5) × 2	2.858(5) × 2
	2.659(9) × 2	2.629(9) × 2
	2.596(8) × 2	2.607(8) × 2
d (La/Li–O2)	3.021(1)	2.994(1)
	2.778(2)	2.763(2)
	2.737(4)	2.737(4)
	2.477(5)	2.500(5)
Mean *d* (La/Li–O)	2.746	2.750
Shannon *d* (La/Li–O)	2.61	2.65
d (Cr/Ti–O1)	1.953(4) × 2	1.949(4) × 2
	1.939(9) × 2	1.947(9) × 2
d (Cr/Ti–O2)	1.959(4) × 2	1.956(4) × 2
Mean *d* (Cr/Ti–O)	1.950	1.951
Shannon *d* (Cr/Ti–O)	2.01	2.01
O1–Cr/Ti–O1	90.5(8) × 2	90.6(7) × 2
	89.5(5) × 2	89.3(3) × 2
O1–Cr/Ti–O2	91.9(6) × 2	90.6(3) × 2
	91.7(1) × 2	90.2(8) × 2
	88.3(5) × 2	89.7(2) × 2
	88.1(3) × 2	89.4(1) × 2
Cr/Ti–O1–Cr/Ti	171.1(6)	169.3(4)
Cr/Ti–O2–Cr/Ti	162.7(3)	165.5(3)
Mean (Cr/Ti–O–Cr/Ti)	166.9	167.4

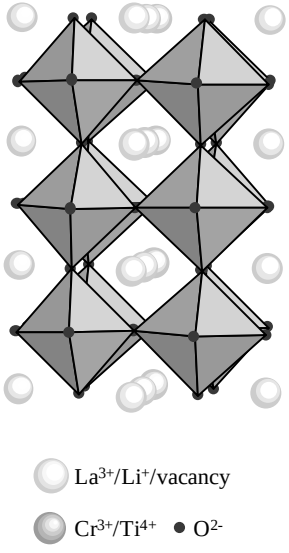

Fig. 3. Structural model of orthorhombic symmetry (S.G.: *Pbnm*).

2.4×10^{-8} F, respectively, are observed at the lowest temperatures. The equivalent circuit used to fit the experimental data is composed of two RC and two constant phase elements (CPEs). These elements (RC and CPE put in serial) are assigned to bulk and grain boundary responses, respectively. At the highest temperature, a spike over the Z'-axis appears and it is reasonable to assume that it is due to the contribution of the electrode.

Conductivity values have been deduced from the intercept of the extrapolated high-frequency first semicircle with the real impedance axis and they can be fitted to an Arrhenius equation of the form $\sigma = (\sigma_0/T)\exp(-E_a/RT)$, as shown in Fig. 5. The activation energy values obtained are relatively low (of about 0.5 eV) and this is indicative that these materials are good conductors. It is observed that the activation energy increases and the conductivity decreases; when the amount of Li and Cr decreases. This fact can be

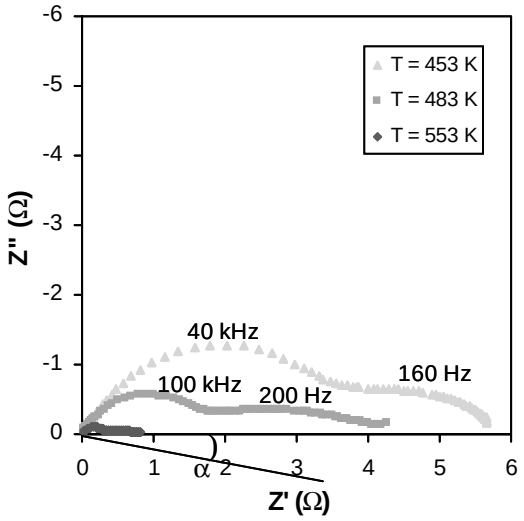

Fig. 4. Complex impedance plots at various temperatures for $La_{1.33}Li_{0.66}Cr_{0.66}Ti_{1.34}O_6$.

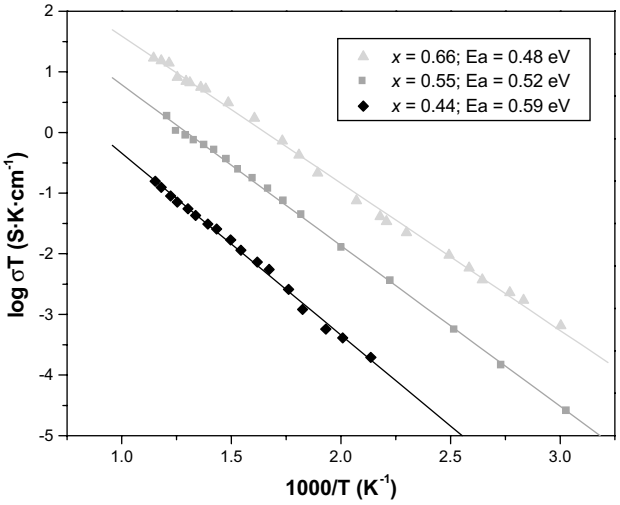

Fig. 5. Arrhenius plots for the system $La_{1.33}Li_xCr_xTi_{2-x}O_6$.

connected with the contribution of ionic conductivity (Li^+) and electronic conductivity (Cr^{3+}). A similar system, described in the bibliography, $La_{1+2x+2y}Li_{1-6x}Ti_{2-6y}Cr_{6y}O_6$ [15,17] shows an electric behavior as mixed conductors.

In order to clarify the nature of charge carriers, electron and/or lithium cations, additional electrical measurements were accomplished [19]. The d.c. polarization technique gives us a qualitative, not quantitative, idea of the carriers that move into the structure. For purely ionic transport, where all the charges passed are stored and released on discharging, the ratio Q_d/Q_c (where Q_d and Q_c are the quantities of charge passed on the discharging and charging mode, respectively) should have the ideal value of unity. In a mixed ionic/electronic conductor, this ratio gives an approximate estimation of the ionic transference number, if one assumes that the reactions occur at the electrode–electrolyte interface during charging. For purely electronic transport, the discharge current could be zero and the ratio Q_d/Q_c must also be zero. The following results of charging/discharging experiments have been interpreted in terms of these hypotheses. The experimental results of charge/discharge processes at 673 K show the ratio Q_d/Q_c low ($\approx 2.0\%$). As it is different from zero, it can be assumed that these materials behave as mixed conductors.

3.3. Magnetic properties

Magnetic measurements have been carried out on all the compositions of this series. Figs. 6 and 7 show the temperature dependence of magnetic susceptibility and its reciprocal for the samples $x = 0.66$, 0.55 and 0.44. To know what is the magnetic behavior of these materials, a close study in the sample with a higher content of chromium ($x = 0.66$) has been carried out. Reciprocal susceptibility data for this compound can be

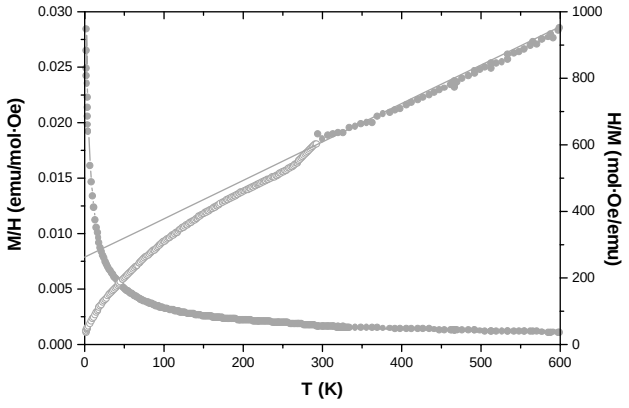

Fig. 6. Magnetic susceptibility and reciprocal susceptibility variations for the sample $La_{1.33}Li_{0.66}Cr_{0.66}Ti_{1.34}O_6$.

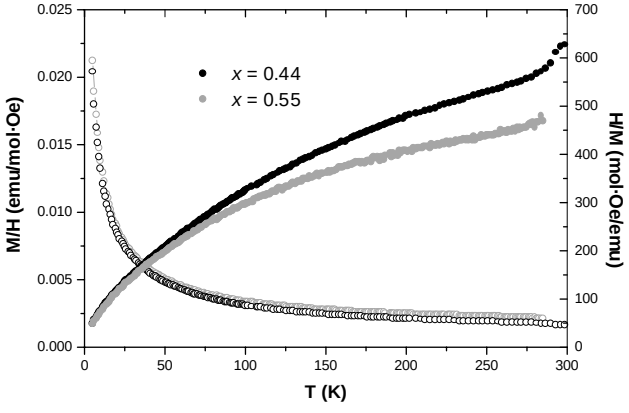

Fig. 7. Magnetic susceptibility and reciprocal susceptibility variations for the system $La_{1.33}Li_xCr_xTi_{2-x}O_6$ for $x = 0.55$ and 0.44 at 5000 Oe.

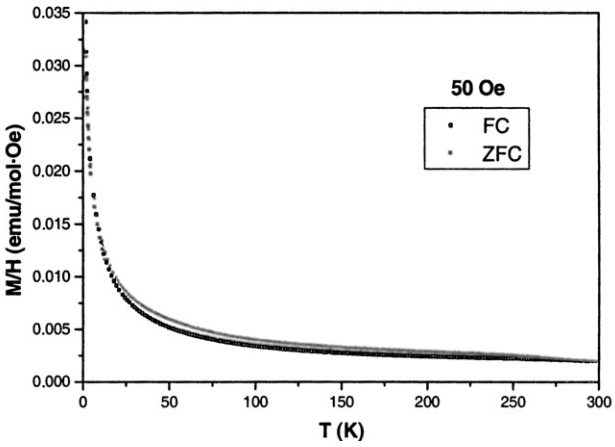

Fig. 8. FC and ZFC M/H vs. temperature for $x = 0.66$ measured with an applied field of 50 Oe.

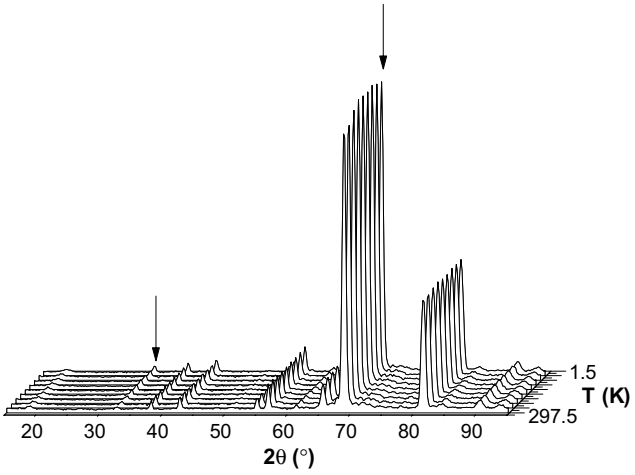

Fig. 9. Neutron thermodiffractograms of $La_{1.33}Na_{0.66}Cr_{0.66}Ti_{1.34}O_6$ between 1.5 and 297.5 K and angular range 15–95°.

fitted to a Curie–Weiss $[M/H = C/(T-\theta)]$ between 300 and 600 K. Experimental magnetic data (2.77 μ_B) is slightly less than the theoretical magnetic data (3.14 μ_B) and this difference can be due to the existence of cooperative magnetic interactions. The negative value of the Weiss parameter (−227 K) could indicate the existence of antiferromagnetic interactions.

Despite, it is usually found the spin glass state in disordered structures and it has been particularly observed in $AB_xB'_{1-x}O_3$ perovskites when some degree of disorder at the B-site is achieved for the magnetic ion [21,24], and although this sample ($x = 0.66$) is magnetically diluted ($Ti^{4+}/Cr^{3+} = 2$), the variation susceptibility vs. temperature has been measured at 50 Oe with ZFC and FC methods and is shown in Fig. 8. A reversible behavior of the ZFC and FC measurements proves that this material does not behave as a spin glass.

Neutron diffraction experiments were performed to confirm the origin of antiferromagnetic interactions. Fig. 9 shows some thermodiffractograms at low temperature and one can note the change of intensity in some maxima ($2\theta \approx 32°$ and 69°), which are marked by arrows in the figure. A similar behavior is observed in the compound $LaCrO_3$ [25,26] and its magnetic structure corresponds to the G-type [27]. An attempt to realise the magnetic structure refinement was not successful due to the magnetic dilution of this sample and hence it is not possible to determinate the direction of spin.

4. Conclusions

The samples of this system present a perovskite-type structure with space group *Pbnm* that is built up by $(Ti/Cr)O_6$ octahedra, which show small tiltings about the direction [001] and [110], and the A-cations (La and Li) and vacancies are distributed at random occupying sites with an anomalous coordination number for the space group *Pbnm*. This behavior can be attributed to the existence of small domains with a local-order structure.

The derivatives of this series present a behavior as mixed conductors because the impedance at low frequency is not a capacitance (non-blocking for the electrons) and the ratio Q_d/Q_c is different from zero. In these materials, the activation energy increases and the conductivity decreases with the value of x. Ionic transport shows that the majority of carriers are electrons, although there is a small number of ionic carriers.

With regard to the magnetic features observed in this series, the reversibility between ZFC and FC measurements, the difference between μ_{exp} and μ_{theo}, the negative Weiss constants and the variation in the intensity of some reflections, suggest an antiferromagnetic ordering beneath 300 K.

Acknowledgments

This work has been done with financial support from the CICYT (MAT 2000-1585-C03-02) and (MAT 2002-01288). A.I.R. is grateful to the Comunidad de Madrid for the fellowship and A.S.B. thanks the Ministerio de Educación, Cultura y Deporte of Spain for financial support under a Postdoctoral Research Fellowship No. EX2001 11787883. We acknowledge the ILL for collecting data of Neutron Diffraction.

References

[1] J. Rodríguez-Carvajal, XV Congress of International Union of Crystallography, Toulouse, FULLPROF, 1990, p. 127.
[2] M.J. MacEarchern, H. Dabkowska, J.D. Garrett, G. Amow, W. Gong, G. Liu, J.E. Greedan, Chem. Mater. 6 (1994) 2092–2102.

[3] I.S. Kim, T. Nakamura, Y. Inaguma, M. Itoh, J. Solid State Chem. 113 (1994) 281–288.
[4] H. Kawai, J. Kuwano, J. Electrochem. Soc. 141 (7) (1994) L78–L79.
[5] J.L. Fourquet, H. Duroy, M.P. Crosnier-López, J. Solid State Chem. 127 (1996) 283–294.
[6] C. León, J. Santamaría, M.A. París, J. Sanz, J. Ibarra, L.M. Torres, Phys. Rev. B 56 (9) (1997) 5302–5305.
[7] J. Emery, J.Y. Buzare, O. Bohnke, J.L. Fourquet, Solid State Ion. 99 (1997) 41–51.
[8] Y. Inaguma, M. Itoh, Solid State Ionics 86–88 (1996) 257–260.
[9] A.I. Ruiz, M.L. López, M.L. Veiga, C. Pico, Solid State Ionics 112 (1998) 291–297.
[10] Y. Inaguma, C. Liguan, M. Itoh, T. Nakamura, T. Uchida, H. Ikuta, M. Wakihara, Solid State Commun. 86 (1993) 689–693.
[11] A.I. Ruiz, M.L. López, M.L. Veiga, C. Pico, J. Solid State Chem. 148 (1999) 329–332.
[12] A.I. Ruiz, M.L. López, M.L. Veiga, C. Pico, Int. J. Inorg. Mater. 1 (1999) 193–200.
[13] A.I. Ruiz, M.L. López, C. Pico, M.L. Veiga, J. Solid State Chem. 163 (2002) 472–478.
[14] M.P. Crosnier-López, H. Duroy, Y. Calage, J.M. Greneche, J.L. Fourquet, Mater. Res. Bull. 36 (2001) 651–671.
[15] M. Morales, L. Mestres, M. Dlouhá, S. Vratislav, M.L. Martínez-Sarrión, J. Mater. Chem. 8 (1998) 2691–2694.
[16] I. Moreno, M. Morales, M.L. Martínez-Sarrión, J. Solid State Chem. 140 (1998) 377–386.
[17] M.L. Martínez-Sarrión, L. Mestres, M. Morales, M. Herraiz, J. Solid State Chem. 155 (2000) 280–285.
[18] M.L. Martínez-Sarrión, L. Mestres, R. Palacín, M. Herraiz, Eur. J. Inorg. Chem. 5 (2001) 1139–1144.
[19] A.I. Ruiz, M.L. López, M.L. Veiga, C. Pico, Eur. J. Inorg. Chem. 4 (2000) 659–664.
[20] A.I. Ruiz, M.L. López, C. Pico, M.L. Veiga, T.A. Ezquerra, Int. J. Inorg. Mater. 3 (2001) 655–659.
[21] A.I. Ruiz, J. Campo, M.L. López, J.L. Martínez-Peña, C. Pico, M.L. Veiga, Eur. J. Inorg. Chem. 5 (2002) 1071–1075.
[22] R.D. Shannon, Acta Crystallogr. A 32 (1996) 751–767.
[23] A.K. Jonscher, Universal Relaxation Law, Chelsea Dielectric Press, London, 1983.
[24] V. Primo-Martín, M. Jansen, J. Solid State Chem. 157 (2001) 76–85.
[25] K. Tezuka, Y. Hinatsu, A. Nakamura, T. Inami, Y. Shimojo, Y. Morii, J. Solid State Chem. 141 (1998) 404–410.
[26] K. Tezuka, Y. Hinatsu, K. Oikawa, Y. Shimojo, Y. Morii, Phys. Cond. Matt. 12 (2000) 4151–4160.
[27] E.F. Bertaut, Acta Crystallogr. A 24 (1968) 217–231.